Chapter 2

Probabilistic Relay Selection Policy

A wide range of relay selection policies exists in the literature on cooperative communication systems. Most of these policies require excessive overhead information exchange between the nodes along with high processing capabilities requirement for the relay nodes. Therefore, to support excessive overhead information exchange and enhanced processing capabilities, highly complex relay nodes are required with increased resource utilization. Such necessities make the system less friendly and less feasible in terms of practical implementation. Therefore in this chapter, we propose

discuss the system model considered in section 2.1. Section 2.2 discusses the proposed relay selection policy and its performance analysis in terms of FASER, FASE, and FAEE. Section 2.3 deals with the diversity order analysis of the system model considered. Lastly, simulation results and summary are presented in section 2.4 and 2.5, respectively. Proofs of all the results discussed in this chapter are relegated in Appendix A.

2.1 System Model and Transmission Protocol

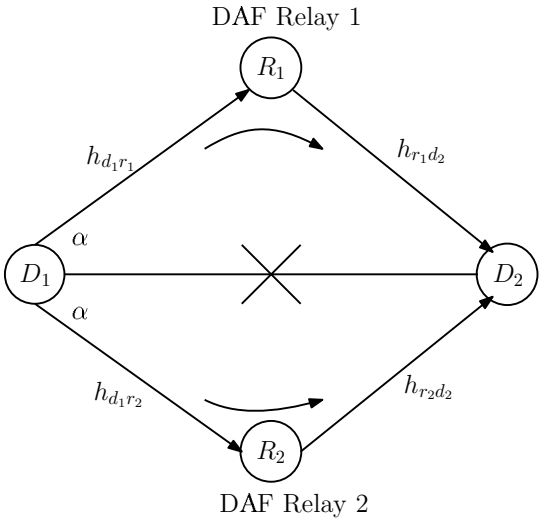

Figure 2.1: DAF relay-assisted, two-hop cooperative D2D system.

A two hop, decode-and-forward (DAF) relay-assisted, cooperative D2D communication system model is shown in figure 2.1. In it, a transmitting device D_1 sends an information symbol α to a receiving device D_2 with the help of a half-duplex DAF relay R_1 or R_2 [96]. We assume that device D_2 is not within the transmission range of D_1, and also there is no direct link between D_1 and D_2 [97]. Therefore, either relay R_1 or R_2 needs to be selected based on a relay selection policy which is described in the next section.

In the cooperative D2D system, each device and relay has a single transmit or receive RF antenna [98]. We assume that all channels undergo frequency-flat Rayleigh fading and are mutually independent [99]. Furthermore, all devices in the system utilize the same bandwidth for their transmissions [96]. To account for path loss, which is due to large scale fading effects, we consider a simplified path loss model [100].

The simplified path loss model: The definition of the simplified path loss model is as follows. Let P_t denote the transmit power of the source node. Suppose that the receiver node is located at some distance d. Then, according to the simplified path loss model, the received signal power is given by [100]

$$P_r = P_t \, \mathcal{K} \left[\frac{d_0}{d} \right]^{\nu},$$

where $\mathcal{K}$ is dimensionless constant dependent on antenna characteristics, d_0 is the reference distance for the antenna far field and ν denotes the path loss exponent. Note that ν lies between 1.6 to 6.5, depending on the propagation environment.

Remarks: Note that the work presented in this thesis focuses on different PHY layer problems, where we focus on optimizing performance measures like FASER, FASE, and FAEE. Our PHY layer system models and their analysis are independent of channel allocation schemes. However, the problems we stated in the thesis can be posed as cross-layer (PHY and medium access control) optimization problems with appropriate assumptions and constraints.

Furthermore, since we analyze bandwidth-normalized channel capacity, the proposed model is generic and applicable to different cooperative D2D or cooperative spectrum sharing communication systems and networks with different bandwidth.

2.1.1 Transmission Protocol for System Model

The cooperative D2D transmission protocol consumes two phases and is illustrated in the table 2.1. In it, α is unit energy information symbol, which is drawn with equal probability from MPSK, P_{d_1} is the transmitting device D_1's transmit power, $h_{d_1 r_j} \sim \mathcal{CN}(0, {\delta_{d_1 r_j}}^2), j = 1, 2$, $h_{r_j d_2} \sim \mathcal{CN}(0, {\delta_{r_j d_2}}^2), j = 1, 2$ are the D_1-R_j channel

Table 2.1: Cooperative D2D transmission protocol.

Phase	Transmission	Reception	Signal expression
Phase 1	D_1transmits	R_j, $j = 1$ or 2	$y_{d_1 r_j} = \sqrt{\tilde{P}_{d_1}} h_{d_1 r_j} \alpha + n_{d_1 r_j}$.
Phase 2	R_j detects and forwards	D_2 receives	$y_{r_j d_2} = \sqrt{\tilde{P}_{r_j}} h_{r_j d_2} \alpha + n_{r_j d_2}$.

gains, and, R_j-D_2 channel gains, respectively. All the additive noise terms are modeled as $\sim \mathcal{CN}(0, \sigma_n^2)$ random variable, and are independent of the channel gains. While $y_{d_1 r_j}, j = 1, 2$ denotes the received signal at the relay, $y_{r_j d_2}$ denotes the received signal at the device D_2.

Received signal powers: Let d_{1r_j} denote the distances between D_1 and $R_j (j = 1, 2)$. Similarly, let $d_{r_j 2}$ denote the distances between $R_j (j = 1, 2)$ and D_2. After accounting path loss, the received signal power at the relay R_j is given by,

$$\tilde{P}_{d_1} = \mathcal{K} P_{d_1} \left[\frac{d_0}{d_{1r_j}} \right]^{\nu}, \tag{2.1.1}$$

where P_{d_1} denote the transmit power of D_1.

The received signal power at D_2 is given by

$$\tilde{P}_{r_j} = \mathcal{K} P_{r_j} \left[\frac{d_0}{d_{r_j 2}} \right]^{\nu}, \tag{2.1.2}$$

where P_{r_j} denote the transmit power of R_1 or R_2.

Generalizations and extensions: While the model that we investigate is qualitatively interesting and insightful, more general cooperative wireless system models are possible. For instance, a model that account for the shadow fading, a large scale fading effect in both the hops. Furthermore, the model can be extended to a system having multiple DAF relays.

Relay selection: We state and derive simple PRSP for different fading scenarios in the following section.

2.2 Selection Policy and FASER Analysis

Our objective is to select a DAF relay that forwards the encoded data symbol to the device D_2. To do so, source node D_1 acquires the average CSI of all the source to relay links. After acquiring this CSI information, the source node will shortlist the best relay node to forward the signal to the destination based on the policy discussed

below. Note that relay node will also need instantaneous CSI, but to decode the received signal properly and not to select the best relay in the system.

DAF relay selection policy proposed is based on partial CSI (one hop). This will reduce the CSI requirement. Specifically, the acquisition of less CSI for channel estimation is less complex than acquiring full CSI. If we consider the second hop channel parameters, the CSI requirement for relay selection will increase significantly, which will obviously enhance the computational complexity of the overall system.

The instantaneous SNR of D_1-R_1 link is given by

$$\Gamma_{R_1} = \frac{\tilde{P}_{d_1} |h_{d_1 r_1}|^2}{{\sigma_n}^2}. \tag{2.2.1}$$

Similarly, The instantaneous SNR of D_1-R_2 link is given by

$$\Gamma_{R_2} = \frac{\tilde{P}_{d_1} |h_{d_1 r_2}|^2}{{\sigma_n}^2}. \tag{2.2.2}$$

Below, we present relay selection policy for different fading scenarios: i) small scale fading with path loss ii) large scale fading with path loss, and iii) both small and large scale fading together with path loss.

2.2.1 Relay Selection Policy: Small Scale Fading with Path Loss

The simple PRSP for small scale fading with path loss is as follows. Select the DAF relay R_1 whenever $\mathcal{P}(\Gamma_{R_1} > \Gamma_{R_2})$. On the other hand, select the DAF relay R_2 whenever $\mathcal{P}(\Gamma_{R_2} > \Gamma_{R_1})$.

Claim 1 *Let* $|h_{d_1 r_1}|^2 \triangleq \gamma_{d_1 r_1}$ *and* $|h_{d_1 r_2}|^2 \triangleq \gamma_{d_1 r_2}$. *Selection of relay* R_1 *occurs with probability* $\mathcal{P}(\Gamma_{R_1} > \Gamma_{R_2}) \triangleq w_1 = \frac{\lambda}{\lambda+\mu}$, *and selection of relay* R_2 *occurs with probability* $\mathcal{P}(\Gamma_{R_2} > \Gamma_{R_1}) \triangleq w_2 = \frac{\mu}{\lambda+\mu}$, *where*

$$\lambda = \frac{\tilde{P}_{d_1} \overline{\gamma}_{d_1 r_1}}{{\sigma_n}^2}, \tag{2.2.3}$$

$$\mu = \frac{\tilde{P}_{d_1} \overline{\gamma}_{d_1 r_2}}{{\sigma_n}^2}, \tag{2.2.4}$$

where $\overline{\gamma}_{d_1 r_1}$, *and* $\overline{\gamma}_{d_1 r_2}$ *denote the average channel power gains of* D_1-R_1, *and* D_1-R_2 *links, respectively. The proof is shown in Appendix A.1.*

Remarks: We note that $\mathcal{P}(\Gamma_{R_1} = \Gamma_{R_2}) = 0$ because of the following reason. $\mathcal{P}(\Gamma_{R_1} = \Gamma_{R_2}) = \int\int_{\mathcal{A}} p_{\Gamma_{R_1}}(u) p_{\Gamma_{R_2}}(v)\, du\, dv$, where $\mathcal{A} = \{(u, v) \in \mathbb{R}^2 : u = v\}$ has

area zero.

Remarks on CSI: In our model, the policy that we propose requires the average CSI for relay selection. Acquiring average CSI is less complex when compared to instantaneous CSI as the latter one requires continuous monitoring of the channel. Furthermore, only the selected DAF relay has to acquire instantaneous CSI for decoding the received signal. Hence, the instantaneous CSI requirement is less when compared to multiple relays cooperating simultaneously to transmit the data to the destination.

In the Rayleigh fading scenario, deriving the relay selection probability is simple, and the probability expression is in closed form. However, we see below that, in other fading scenarios, deriving the relay selection probability is non-trivial and challenging.

2.2.2 Relay Selection Policy: Large Scale Fading with Path Loss

In this fading scenario, we model shadowing, a large scale fading effect, as log-normal random variable, denoted by Ψ. Specifically, we consider the following large scale fading model [100]. Let $Y_1 \sim \mathcal{N}(\mu_1, {\sigma_1}^2)$, and $Y_2 \sim \mathcal{N}(\mu_2, {\sigma_2}^2)$. Further, let $\Gamma_{\Psi R_1} = \frac{\tilde{P}_{d_1}\Psi_1}{{\sigma_n}^2}$, and $\Gamma_{\Psi R_2} = \frac{\tilde{P}_{d_1}\Psi_2}{{\sigma_n}^2}$, where $\Psi_1 = 10^{\frac{Y_1}{10}}$, $\Psi_2 = 10^{\frac{Y_2}{10}}$. Note that the means and variances of Gaussian random variables Y_1 and Y_2 are in dB [100] since they represent power. In this scenario, relay selection policy is as follows.

Claim 2 *Selection of relay R_1 occurs with probability $\mathcal{P}(\Psi_1 > \Psi_2) \triangleq w_{\Psi_1}$, and selection of relay R_2 occurs with probability $1 - \mathcal{P}(\Psi_1 > \Psi_2) \triangleq w_{\Psi 2}$, where*

$$w_{\Psi_1} = \frac{1}{\sqrt{8\pi{\sigma_2}^2}} \int_{-\infty}^{\infty} erfc\left(\frac{y-\mu_1}{\sigma_1\sqrt{2}}\right) \exp\left(-\frac{(y-\mu_2)^2}{2{\sigma_2}^2}\right) dy, \tag{2.2.5}$$

$$w_{\Psi_2} = 1 - w_{\Psi_1}. \tag{2.2.6}$$

where erfc(.) denotes the complementary error function. Proof for the proposed claim is shown in Appendix A.2.

Remarks: In the large scale fading scenario, the expression for relay selection probability is not in closed form. It has a single integral and can be evaluated numerically. We observe that the probability is sensitive to the mean values of the Gaussian random variables.

2.2.3 Relay Selection Policy: Small Scale Plus Large Scale Fading with Path Loss

In this fading scenario, we consider both small scale fading and large scale fading with path loss. Let $\Gamma_{\mathcal{R}\Psi,R_1} = \frac{\tilde{P}_{d_1}\gamma_{d_1r_1}\Psi_1}{{\sigma_n}^2}$, and $\Gamma_{\mathcal{R}\Psi,R_2} = \frac{\tilde{P}_{d_1}\gamma_{d_1r_2}\Psi_2}{{\sigma_n}^2}$. Note that all random variables, namely, $\gamma_{d_1r_1}, \Psi_1$ and $\gamma_{d_1r_2}, \Psi_2$ are statistically independent. Furthermore, all continuous random variables are positive valued. In this scenario, relay selection policy is as follows.

Claim 3 *Selection of relay R_1 occurs with probability $\mathcal{P}(\gamma_{d_1r_1}\Psi_1 > \gamma_{d_1r_2}\Psi_2) \triangleq w_{\mathcal{R}\Psi_1}$, and selection of relay R_2 occurs with probability $1 - \mathcal{P}(\gamma_{d_1r_1}\Psi_1 > \gamma_{d_1r_2}\Psi_2) \triangleq w_{\mathcal{R}\Psi 2}$, where*

$$w_{\mathcal{R}\Psi_1} = \frac{\kappa\overline{\gamma}_{d_1r_1}\overline{\gamma}_{d_1r_2}}{\sqrt{8\pi{\sigma_1}^2}} \int_0^\infty \int_0^\infty \frac{1}{s} erf\left(\frac{\kappa\ln(sz) - \mu_2}{\sigma_2\sqrt{2}}\right) \frac{e^{-\frac{(\kappa\ln s - \mu_1)^2}{2{\sigma_1}^2}}}{\left(s\overline{\gamma}_{d_1r_2} + \overline{\gamma}_{d_1r_1}\right)^2} ds\, dz, \quad (2.2.7)$$

$$w_{\mathcal{R}\Psi_2} = 1 - w_{\mathcal{R}\Psi_1}, \quad (2.2.8)$$

where erf(.) denotes the error function, and $\kappa = \frac{10}{\ln 10}$. Proof for the proposed claim is shown in Appendix A.3.

Remarks: Among the three fading scenarios that we presented above, the expression for relay selection probability in this scenario is the most complex as it contains two integrals. The double integral expression can be evaluated numerically. We can observe that the probability is sensitive to the statistics of small scale fading and also the mean values of the log-normal random variables, which model shadow fading.

2.2.4 FASER Analysis

FASER is the measure to analyze the reliability of the link for signal transmission. It provides information regarding the symbol errors due to noise and channel distortions in the total received symbols at a given point of time. Therefore lower the FASER, higher the reliability of the link. Below we analyze the FASER for the proposed policy.

Let P_{r_1} denote the transmit power of the relay R_1, and P_{r_2} denote the transmit power of relay R_2. After accounting path loss, let $\tilde{P}_{r_1}$ denote the received power at D_2 if R_1 is selected and forwards encoded signal to D_2, and $\tilde{P}_{r_2}$ denotes the received power at D_2 if R_2 is selected and forwards encoded signal to D_2. Furthermore, let Γ_1 denote the received SNR of R_1-D_2 link, and Γ_2 denote the received SNR of R_2-D_2

link. The expressions for Γ_1 and Γ_2 are

$$\Gamma_1 = \frac{\tilde{P}_{r_1} |h_{r_1 d_2}|^2}{{\sigma_n}^2}, \tag{2.2.9}$$

and

$$\Gamma_2 = \frac{\tilde{P}_{r_2} |h_{r_2 d_2}|^2}{{\sigma_n}^2}, \tag{2.2.10}$$

respectively.

For the relay selection policy, we derive FASER, which depends on SNRs of relay to destination links, the rate of selection of relay R_1, and the rate of selection of relay R_2.

Result 1 *Let* $\mathcal{M} \triangleq \sin^2 \frac{\pi}{M}$. *The FASER of MPSK is as follows.*

$$FASER_{MPSK} = 1 - \Bigg[\frac{1}{M} + \frac{w_1 \left(\frac{1}{2} + \frac{1}{\pi} \arctan \left(\sqrt{\frac{1-\mathcal{M}}{\mathcal{M} + \frac{1}{\overline{\Gamma}_1}}} \right) \right)}{\sqrt{1 + \frac{1}{\mathcal{M}\overline{\Gamma}_1}}} + \frac{w_2 \left(\frac{1}{2} + \frac{1}{\pi} \arctan \left(\sqrt{\frac{1-\mathcal{M}}{\mathcal{M} + \frac{1}{\overline{\Gamma}_2}}} \right) \right)}{\sqrt{1 + \frac{1}{\mathcal{M}\overline{\Gamma}_2}}} \Bigg], \tag{2.2.11}$$

where M is the modulation order, $\overline{\Gamma}_1$ denotes the average received SNR if R_1 is selected and forwards the encoded signal, and $\overline{\Gamma}_2$ denotes the average received SNR if R_2 is selected and forwards the encoded signal.

Furthermore, the upper bound for the $FASER_{MPSK}$ is given by

$$FASER_{MPSK} \leq \frac{M-1}{M} \left(\frac{w_1}{1 + \mathcal{M}\overline{\Gamma}_1} + \frac{w_2}{1 + \mathcal{M}\overline{\Gamma}_2} \right) \triangleq FASER_{UB\text{-}MPSK}. \tag{2.2.12}$$

The proof of FASER for MPSK and its upper bound is relegated in Appendix A.4.

Remarks on FASER and its upper bound: The exact FASER and its upper bound are in closed form. The FASER depends on the constellation size, average SNRs of the R_1-D_2 and R_2-D_2 links, and relay selection probabilities. The accuracy of the upper bound is evaluated in Section 2.4.

We now analyze FASER of MQAM. Specifically, we derive FASER expression for MQAM constellations.

Result 2 *Let* $m' \triangleq \frac{3}{2(M-1)}$. *The FASER of MQAM is as follows.*

$$\begin{aligned} FASER_{MQAM} &= 2m\left(1-(w_1M_1+w_2M_2)\right)-m^2 \\ &\quad+\frac{4m^2}{\pi}\left(w_1M_1\cot^{-1}M_1+w_2M_2\cot^{-1}M_2\right), \end{aligned} \tag{2.2.13}$$

where $m=1-\frac{1}{\sqrt{M}}$, $M_1=\sqrt{\frac{m'\overline{\Gamma}_1}{1+m'\overline{\Gamma}_1}}$ *and* $M_2=\sqrt{\frac{m'\overline{\Gamma}_2}{1+m'\overline{\Gamma}_2}}$.

Furthermore, the upper bound for the $FASER_{MQAM}$ *is shown below,*

$$FASER_{MQAM} \leq (2m-m^2)\left[\frac{w_1}{(1+m'\overline{\Gamma}_1)}+\frac{w_2}{(1+m'\overline{\Gamma}_2)}\right] \triangleq FASER_{UB-MQAM}. \tag{2.2.14}$$

Proof for the above mentioned results are derived in Appendix A.5.

2.2.5 FASE Analysis

In addition to FASER, average spectral efficiency also serves as a very useful performance measure. FASE provides information regarding the ability of the cooperative D2D communication system to deliver information rate (in bits per second) for given bandwidth (in Hz). Here, we derive FASE and its upper and lower bound for the proposed policy.

Result 3 *The FASE is given by*

$$\overline{\mathcal{S}}_\eta = \log_2 e\left[w_1\exp\left(\frac{1}{\overline{\Gamma}_1}\right)E_1\left(\frac{1}{\overline{\Gamma}_1}\right)+w_2\exp\left(\frac{1}{\overline{\Gamma}_2}\right)E_1\left(\frac{1}{\overline{\Gamma}_2}\right)\right] \quad bps/Hz. \tag{2.2.15}$$

Furthermore, the average spectral efficiency $\overline{\mathcal{S}}_\eta$ *is both lower bounded and upper bounded as follows.*

$$\overline{\mathcal{S}}_{\eta,l} \leq \overline{\mathcal{S}}_\eta \leq \overline{\mathcal{S}}_{\eta,u}, \tag{2.2.16}$$

where

$$\overline{\mathcal{S}}_{\eta,l} = 0.5w_1\log_2\left(1+2\overline{\Gamma}_1\right)+0.5w_2\log_2\left(1+2\overline{\Gamma}_2\right), \tag{2.2.17}$$

$$\overline{\mathcal{S}}_{\eta,u} = w_1\log_2\left(1+\overline{\Gamma}_1\right)+w_2\log_2\left(1+\overline{\Gamma}_2\right). \tag{2.2.18}$$

Proof for FASE, its upper and lower bond are relegated in Appendix A.6.

2.2.6 Remarks on Energy Efficiency

In the previous section, we analyzed FASE. Another important performance measure, which is closely related to spectral efficiency is energy efficiency. FAEE is defined as the ratio of average spectral efficiency to the total average power consumption [101]. Let $\overline{\mathcal{E}}_\eta$ denote average energy efficiency and $\overline{P}_T$ denote the total power consumption. Mathematically, we have

$$\overline{\mathcal{E}}_\eta = \frac{\overline{\mathcal{S}}_\eta}{\overline{P}_T}. \tag{2.2.19}$$

$\overline{P}_T$ can be considered as the sum of the following three average powers: i). transmit power of source ii). relay's transmit power, and iii). power required for circuitry. Here, we do not present a detailed analysis of average energy efficiency. Our model can be extended, and new problem formulations on the optimization of energy efficiency are possible.

In the following section, we present diversity order analysis. In it, we derive the diversity order of the proposed relay selection policy in a scaling regime.

2.3 Diversity Order Analysis

The significance of diversity order is that it provides valuable analytical insights regarding the robustness of the proposed relay selection policy against fading effects, such as small scale fading and large scale fading. Let p_e, a function of the received signal SNR, denote the probability of error. In simple terms, it is defined as the exponent of SNR in the following.

$$p_e \propto \frac{1}{\mathrm{SNR}^L},$$

where L denotes the diversity order [102].

We now prove that the diversity order of the relay selection policy is one for Rayleigh fading in the following scaling regime: $\overline{\Gamma}_1$ and $\overline{\Gamma}_2$ are very high, but finite, and $\overline{\Gamma}_1 \approx \overline{\Gamma}_2$. Note that all other parameters, such as, constellation size M, w_1, and, w_2 are fixed. We state the following result on the diversity order.

Result 4 *Let the diversity order is denoted by d_{PRSP}. The diversity order d_{PRSP} is equal to 1 for Rayleigh fading.*

Proof of the above result is given in A.7.

Note that the diversity order of 1 is due to the fact that we are using single antenna nodes and the direct path is absent. However, the diversity order can be increased by

using multiple antennas at the DAF relay and/or destination. For example, by using the simple transmit diversity scheme, that is, the Alamouti scheme, diversity order can be increased. Since the analysis of multiple antenna system is out of the scope of this work, we will not discuss it further.

2.4 Results, and Discussion

We now numerically evaluate the performance of proposed relay selection policy and verify the analytical results using Monte Carlo simulations that use up to 10^5 samples. In all plots, we assume that ${\sigma_n}^2 = 1$, and path loss exponent $\nu = 2.7$. Note that the value of path loss exponent depends on the propagation environment [100]. To numerically investigate the impact of path loss exponent on our system performance, we have chosen $\nu = 2.7$, since this value is valid for the urban micro-cell environment [100]. However, the analytical results we derived are valid for any value of ν. Also, let d denotes the distance between the relay node and destination device and d_0 be the reference distance for the antenna far field.

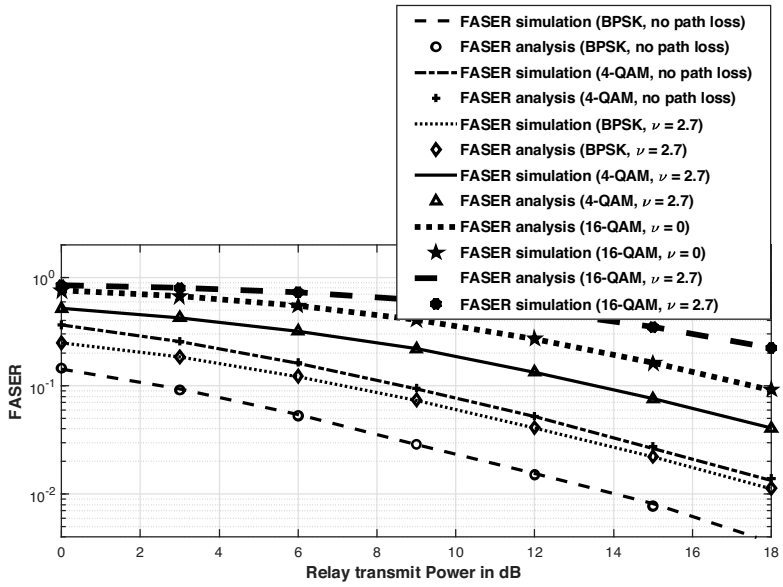

Figure 2.2: FASER as a function of relay transmit power (Mean channel power gains of all links = 1, ${\sigma_n}^2 = 1$, $\mathcal{K} = 0$ dB, $d_0 = 100$ m, and $d = 150$ m.).

Figure 2.2 plots FASER as a function of relay transmit power for BPSK, 4-QAM and 16-QAM constellations, and for i) without and ii) with path loss. In simulation, we set $P_{r_1} = P_{r_2} = P_r$ and all mean channel gains are fixed to unity. We observe that as relay transmit power increases, FASER decreases. However, at higher order modulations, FASER is high, as expected. Furthermore, the presence of path loss further degrades the FASER performance.

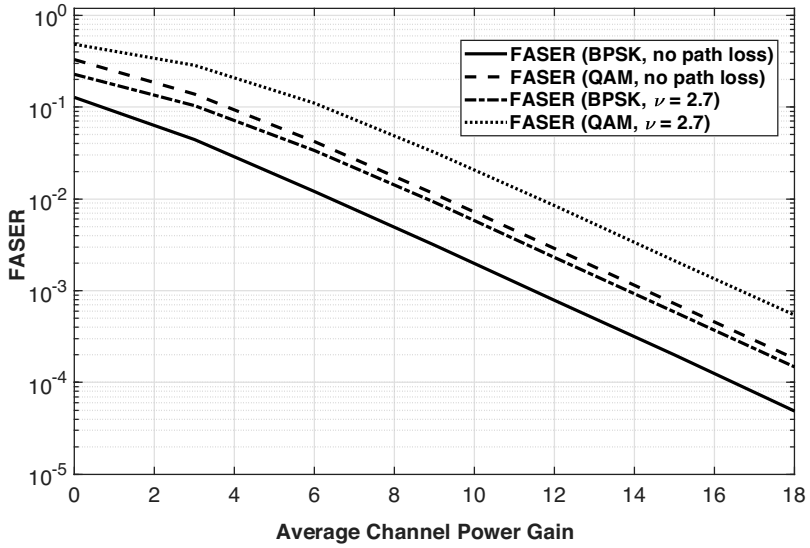

Figure 2.3: FASER as a function of mean channel power gain ($P_{r_1} = P_{r_2} = 1$ dB, ${\sigma_n}^2 = 1$, $\mathcal{K} = 0$ dB, $d_0 = 100$ m, and $d = 150$ m.).

Figure 2.3 plots FASER as a function of mean channel power gain for BPSK and 4-QAM constellations, and for i) without and ii) with path loss. In it, relay transmit power is fixed at 1 dB. We observe that as average channel power gain increases, FASER decreases. This is because, stronger channel links cause improved received SNRs. We observe that QAM delivers inferior FASER performance when compared with BPSK, as expected. Furthermore, the presence of path loss further degrades the average symbol error rate performance.

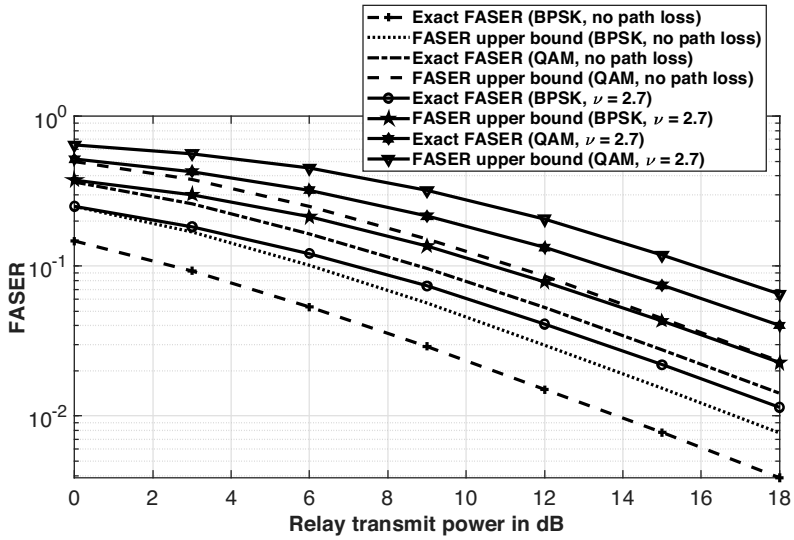

Figure 2.4: FASER and its upper bound as a function of relay transmit power (Mean channel power gains of all links = 1, ${\sigma_n}^2 = 1$, $\mathcal{K} = 0$ dB, $d_0 = 100$ m, and $d = 150$ m.).

Figure 2.4 plots FASER and its upper bound as a function of relay transmit power for BPSK and 4-QAM constellations, and for i) without and ii) with path loss. In simulations, we set $P_{r_1} = P_{r_2} = P_r$ and all mean channel gains are fixed to unity. We observe that the upper bound tracks the exact FASER well. While it is a loose upper bound for BPSK, it becomes tighter in the path loss scenario.

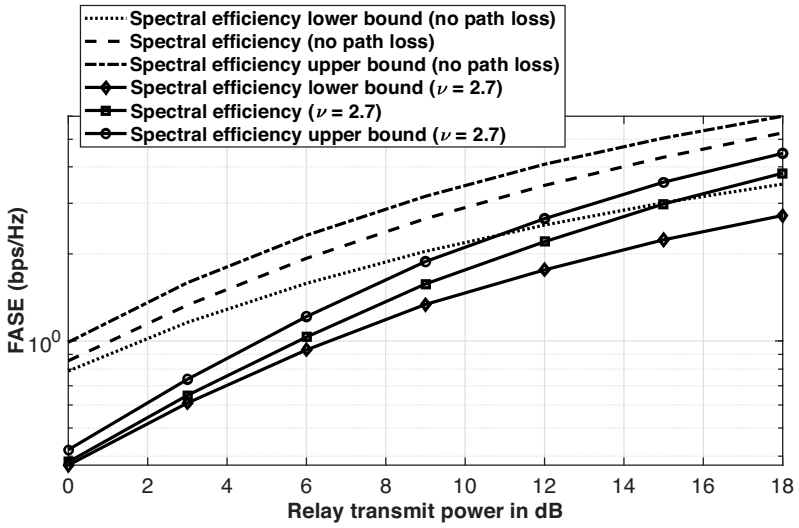

Figure 2.5: Average spectral efficiency and its bounds as functions of relay transmit power (Mean channel power gains of all links = 1, ${\sigma_n}^2 = 1$, $\mathcal{K} = 0$ dB, $d_0 = 100$ m, and $d = 150$ m.).

Figure 2.5 plots FASE and its bounds as a function of relay transmit power for i) without and ii) with path loss. In simulations, we set $P_{r_1} = P_{r_2} = P_r$ and all mean channel gains are fixed to unity. We observe that as relay transmit power increases, average spectral efficiency increases. This is because, strong relay to destination links cause improved received SNRs. Furthermore, the presence of path loss further degrades the average spectral efficiency performance.

Figure 2.6 plots FAEE and its bounds as a function of relay transmit power for i) without path loss, and ii) with path loss. We set $P_{r_1} = P_{r_2} = P_r$ and all mean channel gains are set to unity. We observe that as relay transmit power increases, average energy efficiency decreases. This is because of the fact that the total average power consumption increases. Furthermore, we see that the presence of path loss degrades the average energy efficiency performance, as expected.

Figure 2.7 plots FASER as a function of relay transmit power for two different relay selection policies, that is, opportunistic relay selection policy (ORSP) [56, 103] and PRSP. From figure 2.7, we see that the PRSP performs better than ORSP for both BPSK and 4-QAM constellation schemes. Table 2.2 compares the proposed PRSP

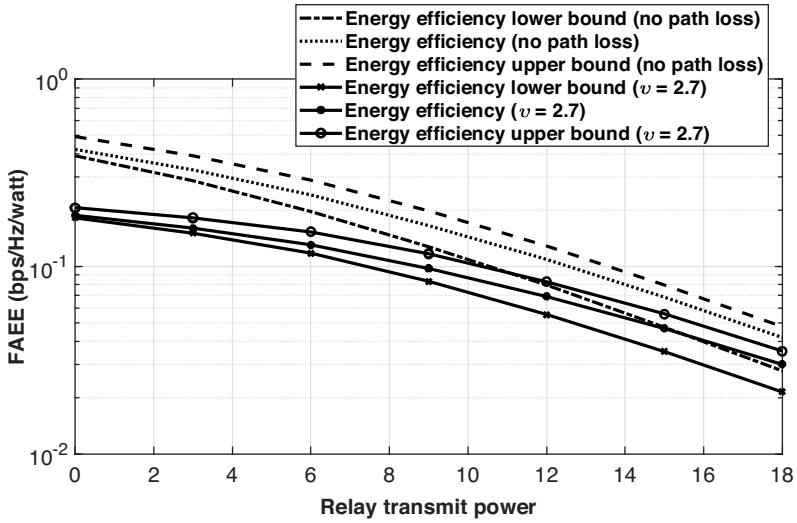

Figure 2.6: Average energy efficiency and its bounds as functions of relay transmit power (Circuitry Power $P_c = 15$ dBm, Mean channel power gains of all links $= 1$, ${\sigma_n}^2 = 1$, $\mathcal{K} = 0$ dB, $d_0 = 100$ m, and $d = 150$ m.).

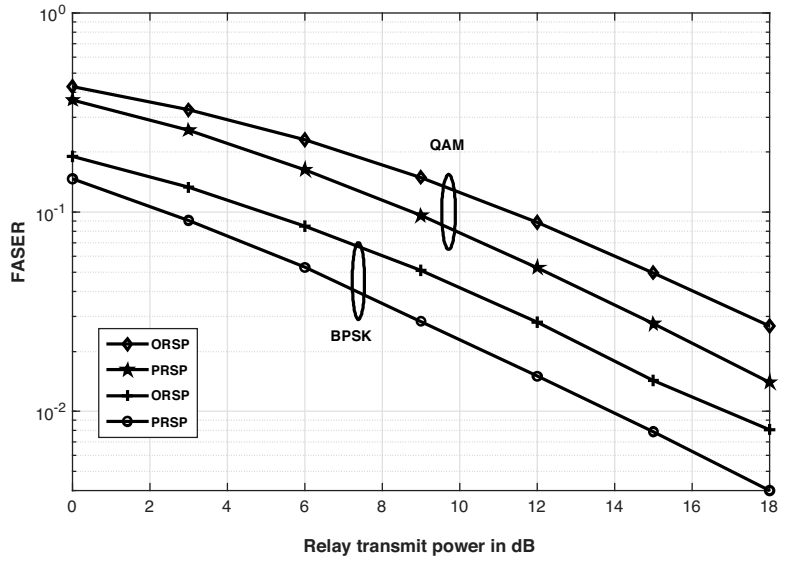

Figure 2.7: FASER as a function of relay transmit power for ORSP and PRSP (Mean channel power gains of all links $= 1$, ${\sigma_n}^2 = 1$.).

and the benchmark policy ORSP. Note that for fair a comparison with ORSP, we do not consider the direct path and also the use of space-time coding for a diversity-multiplexing tradeoff.

Remarks on performance comparison of PRSP and ORSP: Note that for analyzing FASER expression in high SNR regime, we have assumed mean channel power gain of all links to be same and equal to $\overline{\gamma}$ and the relay transmit power $P_r \to \infty$. From the

Table 2.2: Performance comparison of PRSP and ORSP in high SNR regime.

Policy	PRSP	ORSP
FASER Expression for High SNR Regime	$\text{FASER}^{\text{H}}_{\text{PRSP}} = \left[\frac{K}{\pi\mathcal{M}}\right]\left[\frac{1}{\overline{\Gamma}^1}\right]$, where $\overline{\Gamma}^1$ is the mean received SNR and $K = \left(\frac{M-1}{2M}\right)\pi - \frac{\sin\left(\frac{M-1}{M}\right)2\pi}{4}$.	$\text{FASER}^{\text{H}}_{\text{ORSP}} = \left[\frac{4K}{3\pi\mathcal{M}}\right]\left[\frac{1}{\overline{\Gamma}^1}\right]$.
Diversity Order	One.	One.

expressions shown in table 2.2 it can be observed that the $\text{FASER}^{\text{H}}_{\text{ORSP}}$ is $\frac{4}{3}$ times higher than $\text{FASER}^{\text{H}}_{\text{PRSP}}$. In other words, PRSP outperforms ORSP in terms of FASER. It can also be observed that diversity order for both the policy is one. However, PRSP achieves diversity order of one faster. The proof of the above FASER expressions in high SNR regime for PRSP and ORSP is shown in appendix A.8 and appendix A.9, respectively.

2.5 Summary

This chapter proposed a simple PRSP for a four-node cooperative, DAF relay-assisted D2D wireless communication system over different fading scenarios in the first hop. We further investigated FASER for the proposed relay selection scheme, taking a small scale fading scenario with path loss. Specifically, we derived closed-form expressions of FASER for two different constellations: MPSK and MQAM. In addition to error analysis, we analyzed FASE and FAEE. We extended our analysis and presented an insightful result on diversity order analysis. To further enhance the performance of the system model considered, we propose a hybrid relaying policy with PRSP in the next chapter.